

Electronic Supplementary Information (ESI)

Matter, energy and information network of graphene-peptide-based fluorescent sensing system for molecular logic computing, detection and imaging of cancer stem cell marker CD133 in cells and tumor tissues

Fu Rui Zhang,[#] Jiao Yang Lu,[#] Qing Feng Yao, Qiu Yan Zhu, Xin Xing Zhang, Wei Tao Huang,* Li Qiu Xia and Xue Zhi Ding*

State Key Laboratory of Developmental Biology of Freshwater Fish, Hunan Provincial Key Laboratory of Microbial Molecular Biology, College of Life Science, Hunan Normal University, Changsha 410081, P. R. China.

*Corresponding author:

E-mail: vthuang@hunnu.edu.cn. Fax: (+86)731-8887-2905; Tel: (+86)731-8887-2905

E-mail: dingxuezhi@hunnu.edu.cn. Fax: (+86)731-8887-2905; Tel: (+86)731-8887-2905

[#] These authors contributed equally to this work.

1. The chemical structure of the CD133-binding peptide FLS7.

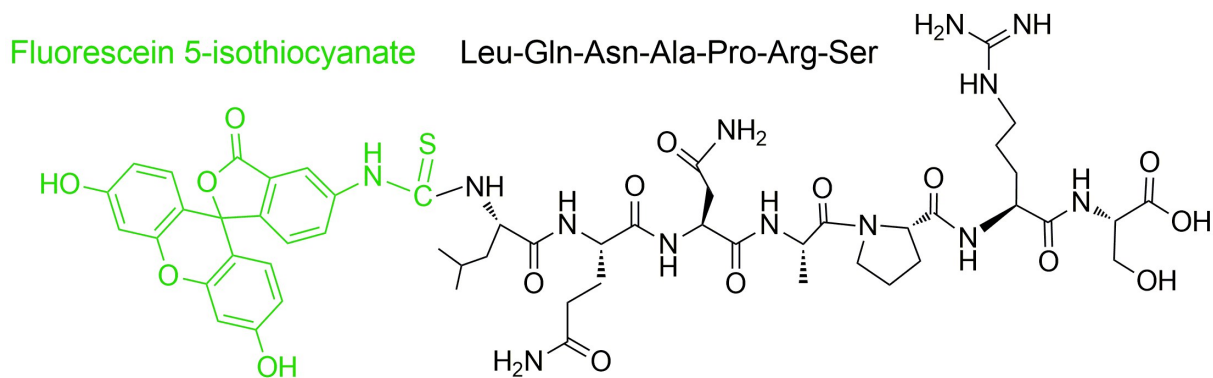


Figure S1. The chemical structure of the CD133-binding peptide FLS7.

2. Quenching mechanism of GO and FLS7 peptide.

To further confirm quenching mechanism, the Stern–Volmer constant (K_{SV}) of GO to FLS7 was calculated at different temperatures according to the equation:

$$F_0/F = 1 + K_{SV} [\text{quencher}] \quad (1)$$

F_0 and F are the fluorescence intensities of FLS7 in the absence and presence of GO, respectively. The values of K_{SV} (0.2841 mL/ μ g at 25°C, 0.1613 mL/ μ g at 35°C, 0.1485 mL/ μ g at 45°C) decreased with increase in temperatures (Figure S2D), indicating the formation of the static quenching complex between GO and FLS7. Since the molar concentration of GO cannot be estimated due to its polydispersity, a K_{SV} value is represented in mL/ μ g. The static quenching constant (K_p) at 25°C was 0.0658 mL/ μ g calculated according to the equation:

$$\ln(F_0/F) = K_p [\text{quencher}] \quad (K_p \text{ is the Perrin constant}) \quad (2)$$

The binding constant K_A at 25°C was 0.4740 mL/ μ g calculated according to the equation:

$$\text{Log}(F_0 - F)/F = \text{log}K_A + \text{nlog}[\text{quencher}] \quad (3)$$

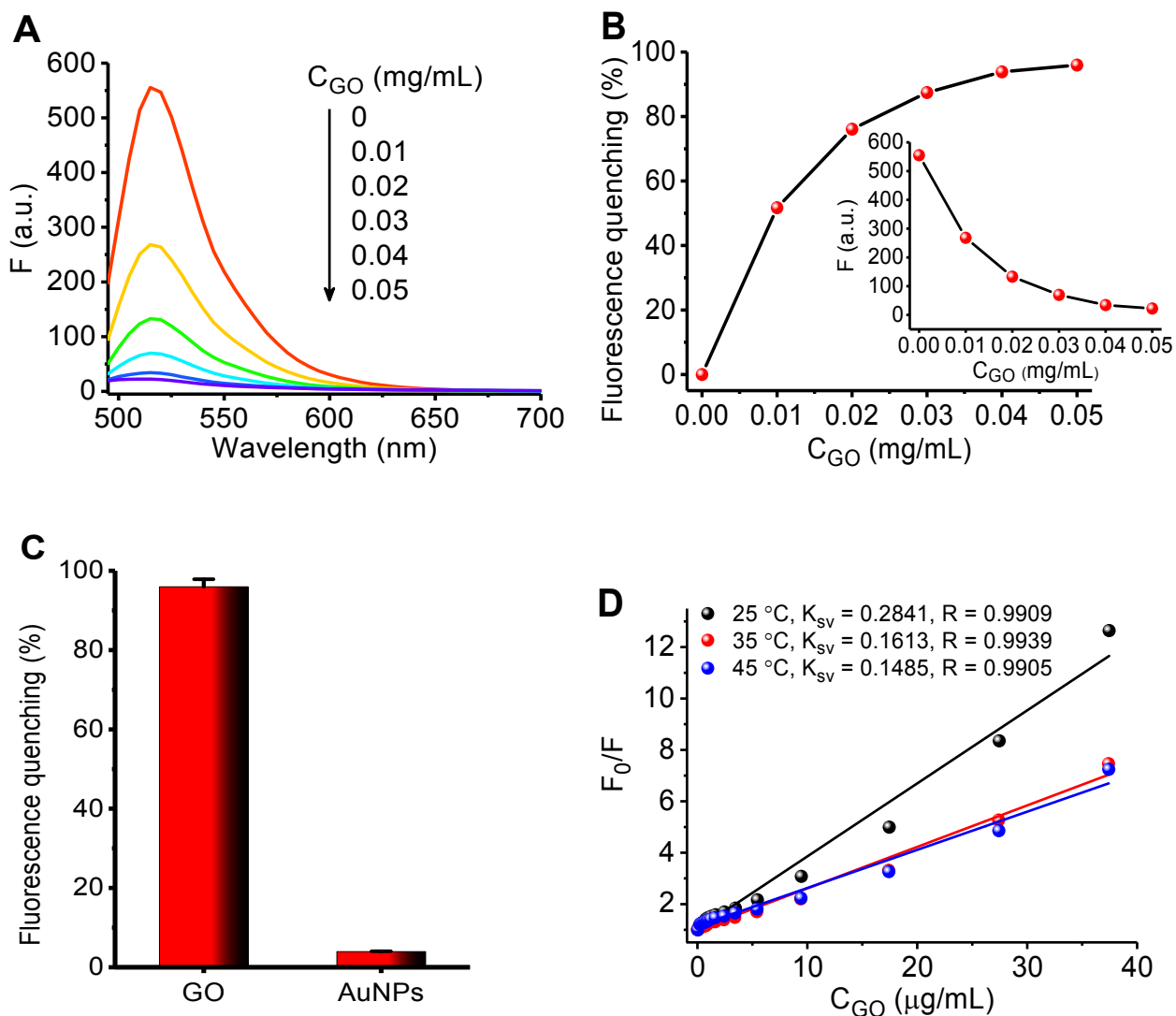


Figure S2. (A) The fluorescence emission spectra of FLS7 (100 nM) solutions titrated with different concentrations of GO. (B) Dependence of fluorescence quenching ratio $(F_0 - F)/F_0$ of FLS7 as a function of C_{GO} used for titration. Inset: Dependence of fluorescence intensity of FLS7 as a function of C_{GO} . (C) Comparison of fluorescence quenching abilities of GO and AuNPs. Buffer: 25 mM Tris-HCl, pH 7.4. (D) Stern-Volmer plot for the binding of FLS7 with GO at 25, 35 and 45 °C.

3. Measurement of binding affinity of the FLS7 for CD133 by using fluorescence anisotropy.

The purified CD133 proteins at increasing concentrations were added into the FLS7 (10 nM) solution. Then the reaction solution was allowed to equilibrate for 10 min and analyzed with a SpectraMax M5 microplate spectrophotometer system (Molecular Devices, USA) in a fluorescence anisotropy mode. Anisotropy (r) was calculated as $r = (I_{VV} - G \times I_{VH}) / (I_{VV} + 2 \times G \cdot I_{VH})$, where I_{VV} is the fluorescence intensity with vertically oriented excitation and emission polarizers, I_{VH} is the fluorescence intensity with a vertically oriented excitation polarizer and a horizontally oriented emission polarizer, and the G-factor, defined as $G = I_{HV} / I_{HH}$, was set to 1.0 in all experiments. K_d values were calculated by fitting curves of anisotropy versus protein concentration to a standard single-site binding equation $r = B_{\max} \times [S] / (K_d + [S])$ using Origin (OriginLab).

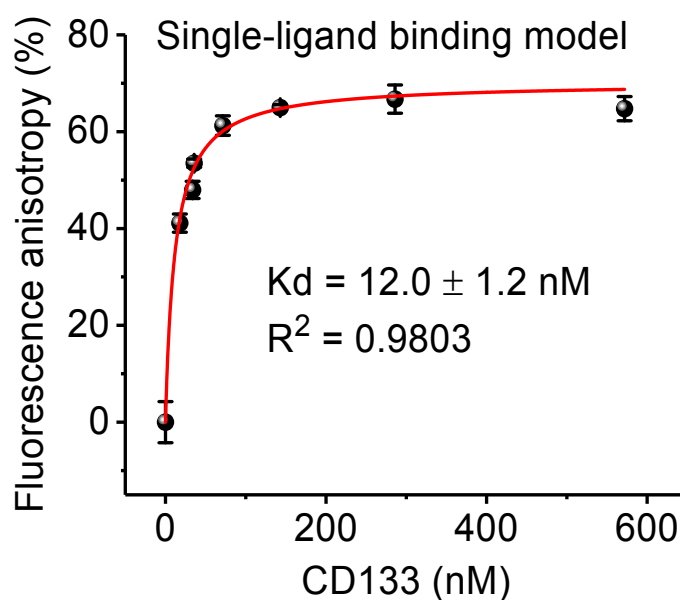


Figure S3. Change in fluorescence anisotropy versus [CD133] is plotted (solid circles) and fit to a single-ligand binding model (red line). FLS7, 10 nM; CD133, 0 to 572 nM; Buffer: 25 mM Tris-HCl, pH 7.4.

Table S1. Comparison of binding affinity of different CD133-binding probes.

	Name	Binding affinity (K_d , nM)	Target
Peptides	CBP4 ^[1]	5.5	CD133 protein
	CP ^[2]	7.37	CD133 protein
	FLS7	12.0	CD133 protein
Aptamers	RNA A15 ^[3]	83.2	CD133 ⁺ HT-29 cells ^a
		33.9	CD133 ⁺ Hep3B cells
	RNA B19 ^[3]	145.1	CD133 ⁺ HT-29 cells
		52.3	CD133 ⁺ Hep3B cells
Antibody ^[1]	4.1	CD133 protein	

^a CD133 positive is represented as CD133⁺.

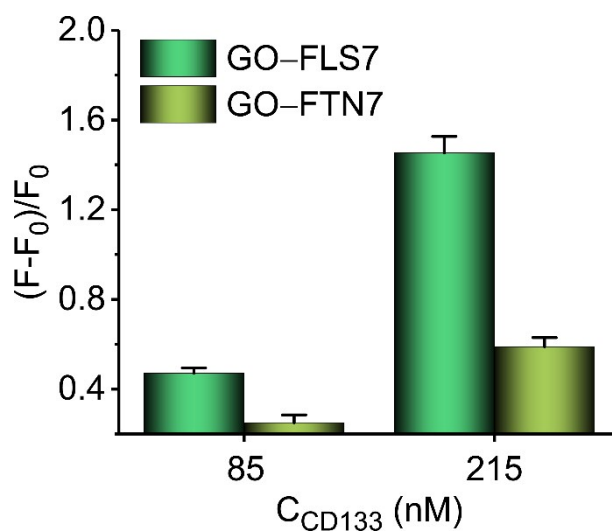


Figure S4. Comparison of fluorescence response of the CD133-binding peptide FLS7 and the control peptide FTN7 (FITC-TNTLSNN) to CD133 when two peptides were adsorbed with the GO.

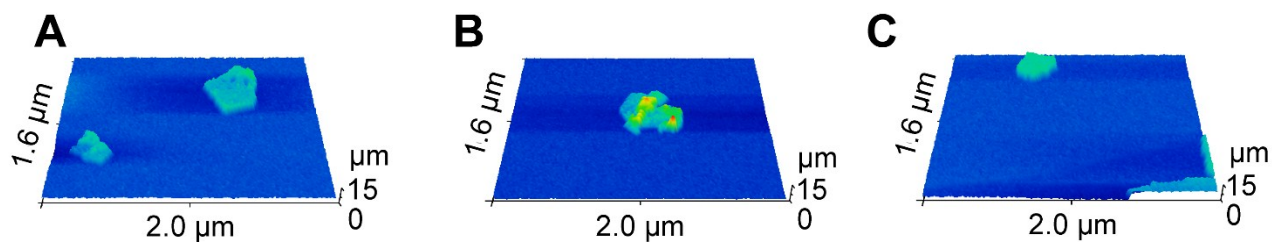


Figure S5. 3D AFM images of GO (A), GO-FLS7 complex (B), and GO-FLS7-CD133 mixture (C).

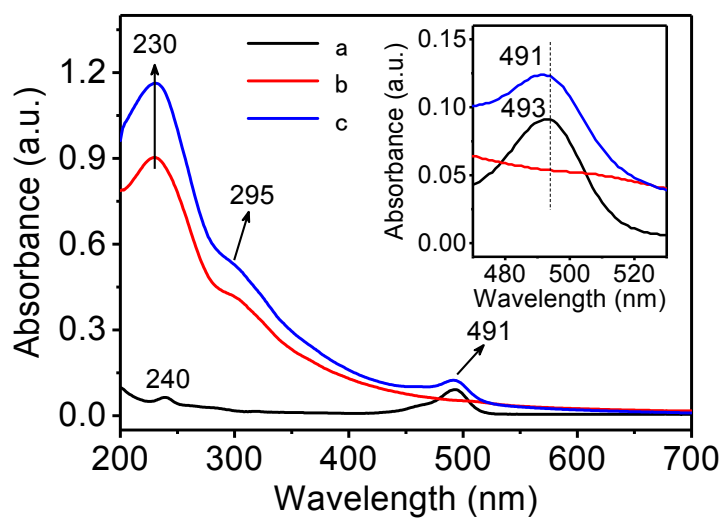


Figure S6. UV-Vis absorption spectra of FLS7 (a), GO (b), GO-FLS7 complex (c). The solvents were 25 mM Tris-HCl, pH 7.4.

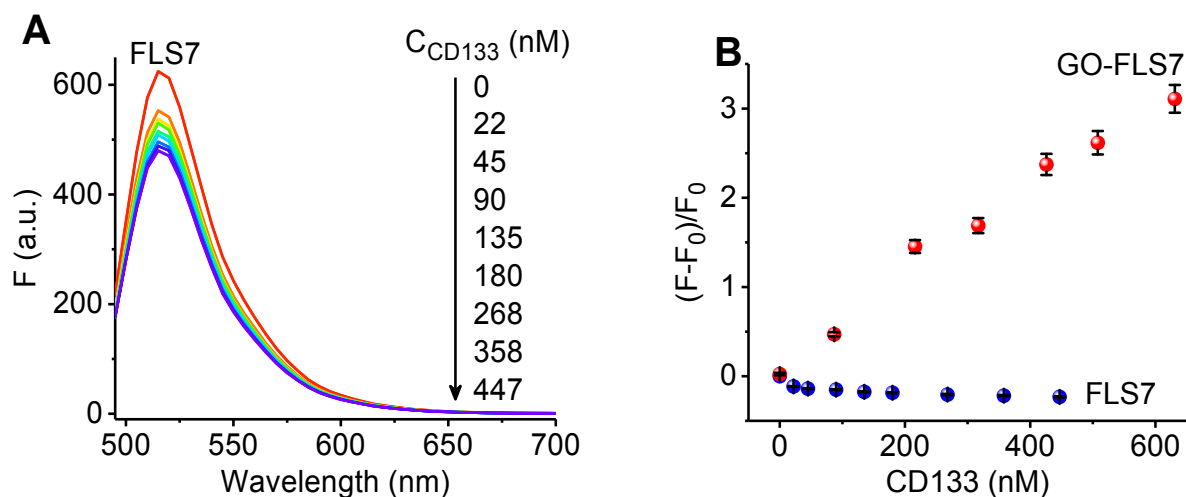


Figure S7. (A) Fluorescence emission spectra of FLS7 (100 nM) upon addition of different concentrations of CD133 (from top to bottom: 0, 22, 45, 90, 135, 180, 268, 358, 447 nM). (B) Comparison of the fluorescence responses $(F-F_0)/F_0$ of FLS7 (blue dots) and GO-FLS7 complex (0.05 mg/mL:100 nM, red dots) to the different concentrations of CD133.

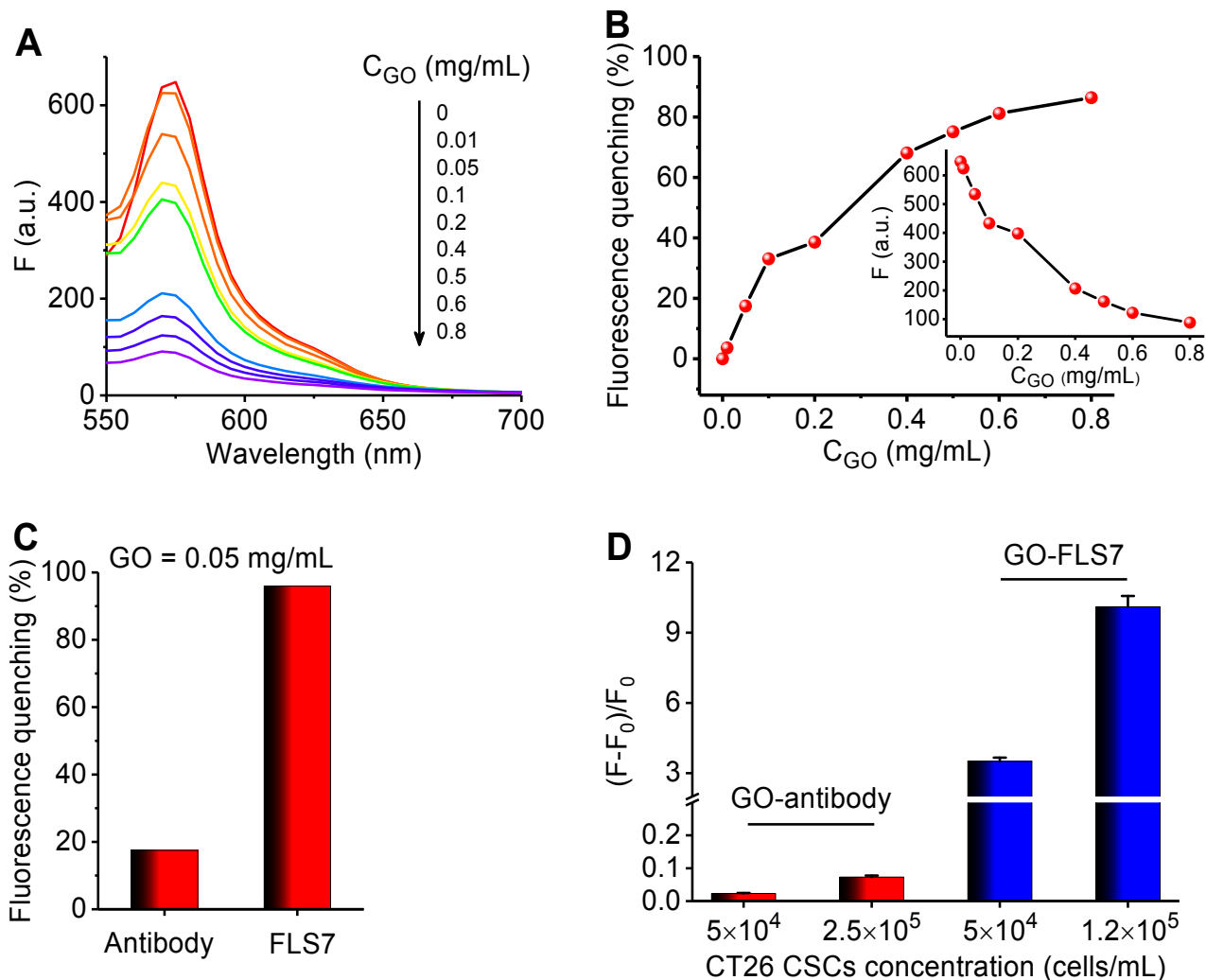


Figure S8. (A) The fluorescence emission spectra of phycoerythrin-labeled CD133 monoclonal antibody (PE-CD133 MAb, 0.25 $\mu\text{g/mL}$) solutions titrated with different concentrations of GO. (B) Dependence of fluorescence quenching ratio $(F_0 - F)/F_0$ of PE-CD133 MAb as a function of C_{GO} used for titration. Inset: Dependence of fluorescence intensity of PE-CD133 MAb as a function of C_{GO} . (C) Comparison of fluorescence quenching abilities of GO to PE-CD133 MAb and FLS7 peptide. (D) Comparison of fluorescence responses of GO-antibody (0.8 mg/mL: 0.25 $\mu\text{g/mL}$) and GO-FLS7 (0.05 mg/mL: 100 nM) to CT26 CSCs. Buffer: 25 mM Tris-HCl, pH 7.4.

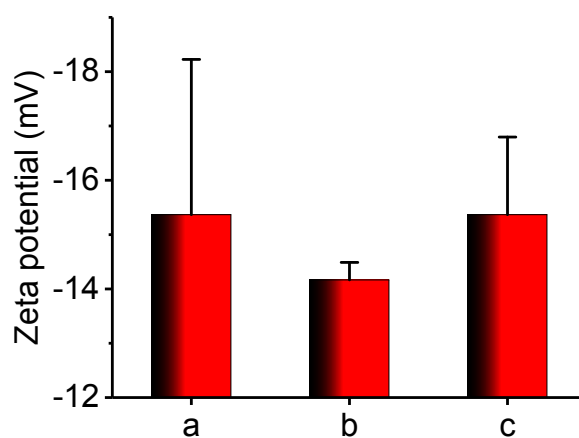


Figure S9. Comparison of zeta potential of GO (a), GO-FLS7 complex (b), and GO-FLS7-CD133 mixture (c). Concentrations: GO (2 mg/mL), FLS7 (4.03 μ M), CD133 (894 nM).

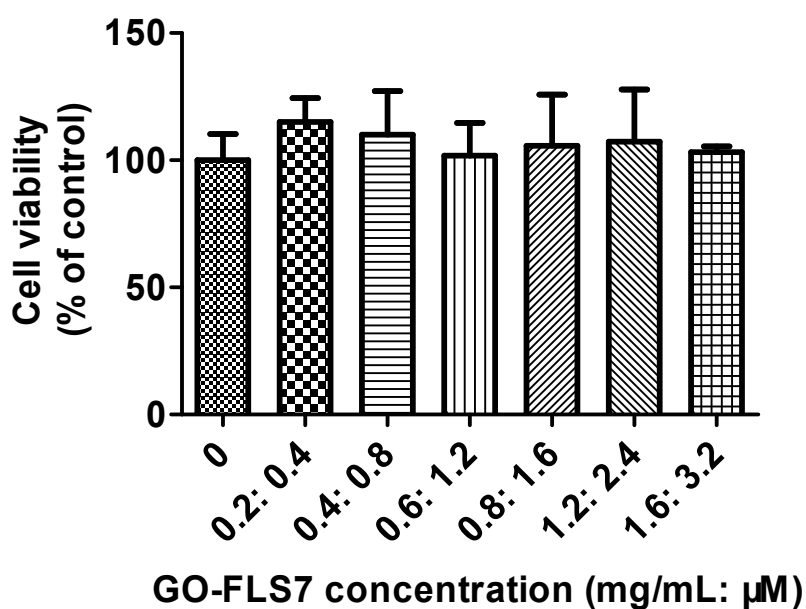


Figure S10. The cell viability of CT26 cells after exposed to GO-FLS7 complex for 24 h.

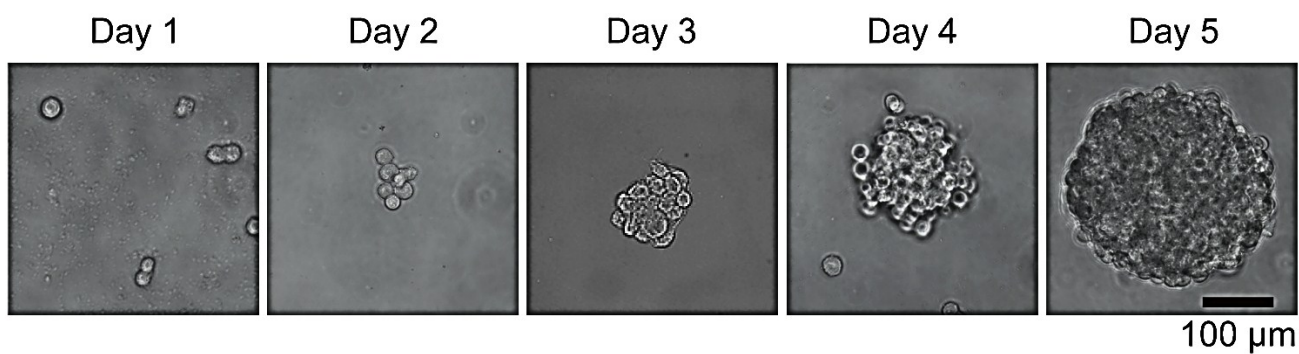


Figure S11. Optical microscopy images of CT26 CSCs tumor sphere formation process by using the serum-free suspension culture method. Scale bar, 100 μm for all images.

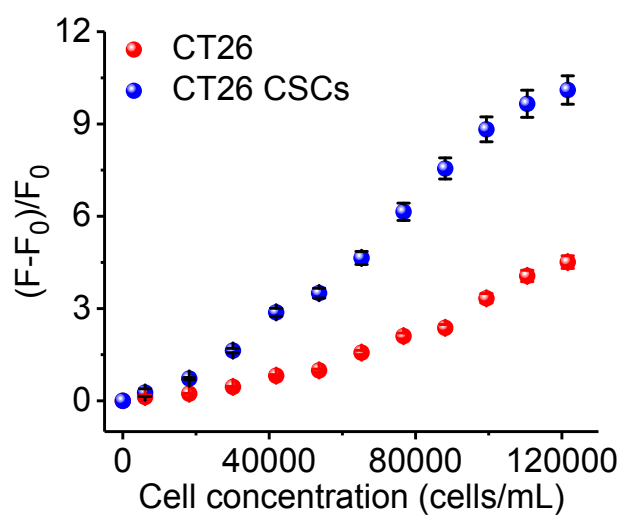


Figure S12. Comparison of the fluorescence changes of GO-FLS7 nanoprobes (0.05 mg/mL:100 nM) on the different concentration of CT26 CSCs and CT26 cells.

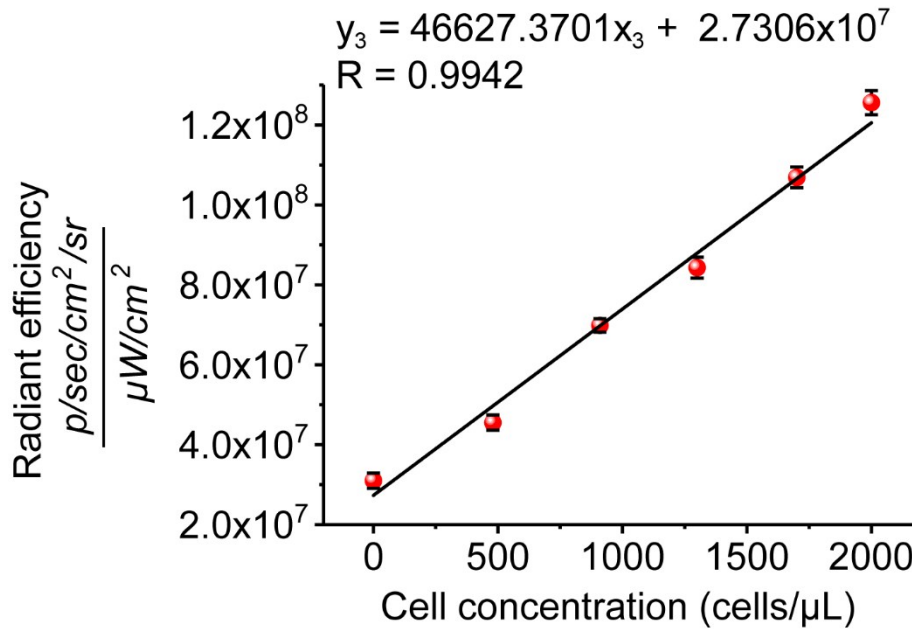


Figure S13. The quantitative analysis of fluorescent images of the mixtures of GO–FLS7 nanoprobes and different concentrations of CT26 CSCs.

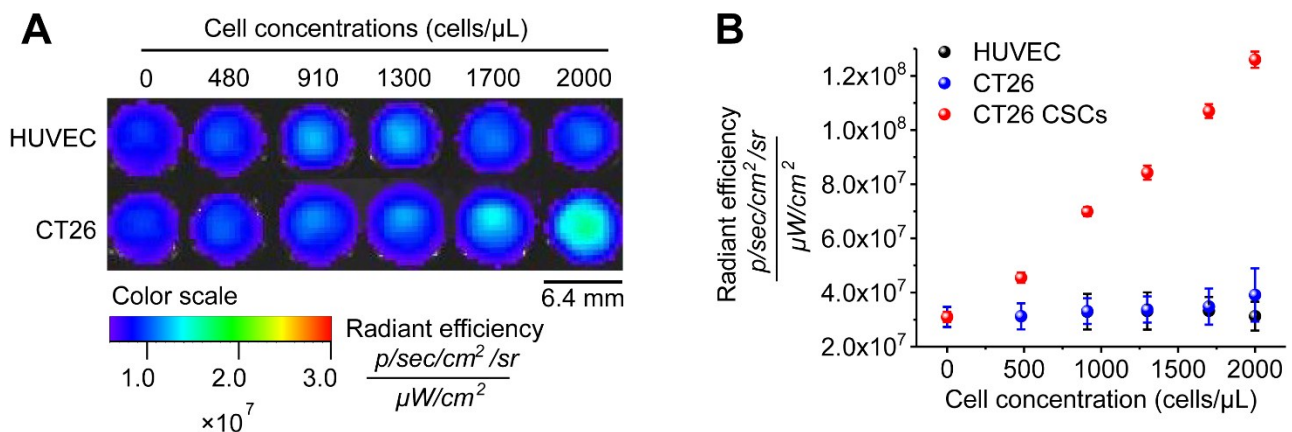


Figure S14. (A) In vitro fluorescent images of the GO–FLS7 nanoprobes upon addition of different concentrations of CT26 or HUVEC. Scale bar, 6.4 mm. (B) Comparison of their quantitative analysis of fluorescent images of the GO–FLS7 nanoprobes to CT26 CSCs, CT26, and HUVEC according to Figure S14A and Figure 4E.

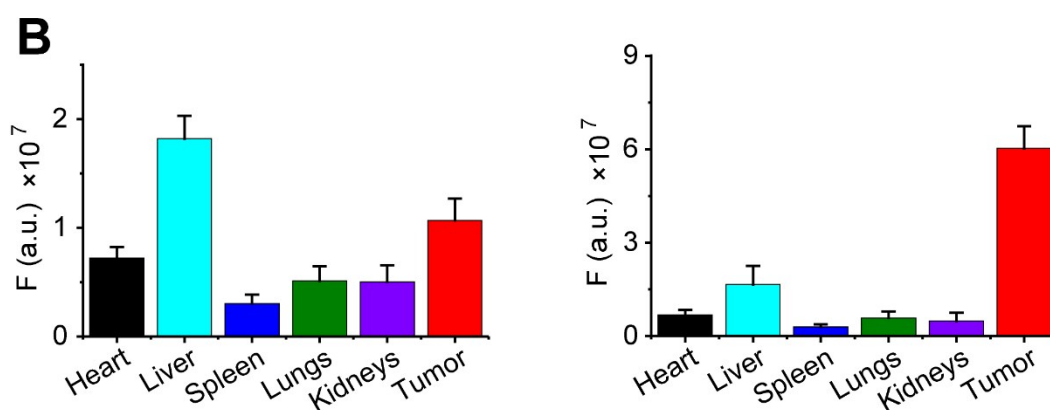
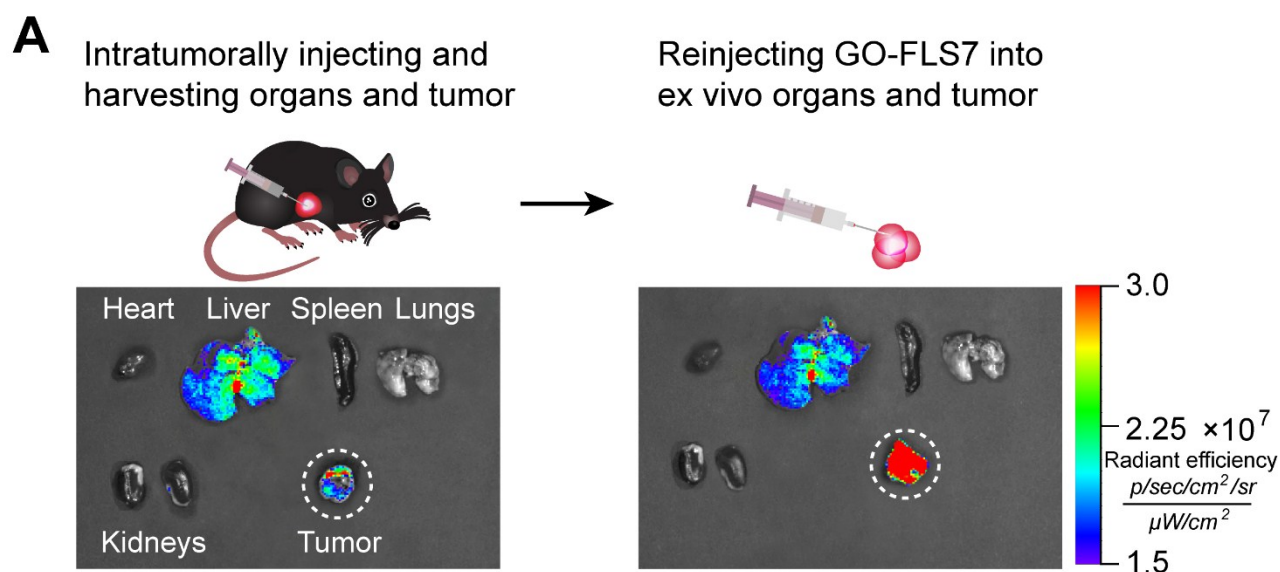


Figure S15. (A) Comparison of representative fluorescence images of ex vivo main organs (heart, liver, spleen, lungs, and kidneys) and tumor of tumor-bearing mice treated with GO-FLS7 complex at 2 h post-intratumoral injection (left) and at 30 min post-reinjection of GO-FLS7 complex into ex vivo organs and tumor (right). (B) Comparison of fluorescence intensity of ex vivo organs and tumor at 2 h post-intratumoral injection (left, $n = 3$ samples) and at 30 min post-reinjection of GO-FLS7 complex (right, $n = 3$ samples). The results are presented as the mean \pm s.d.

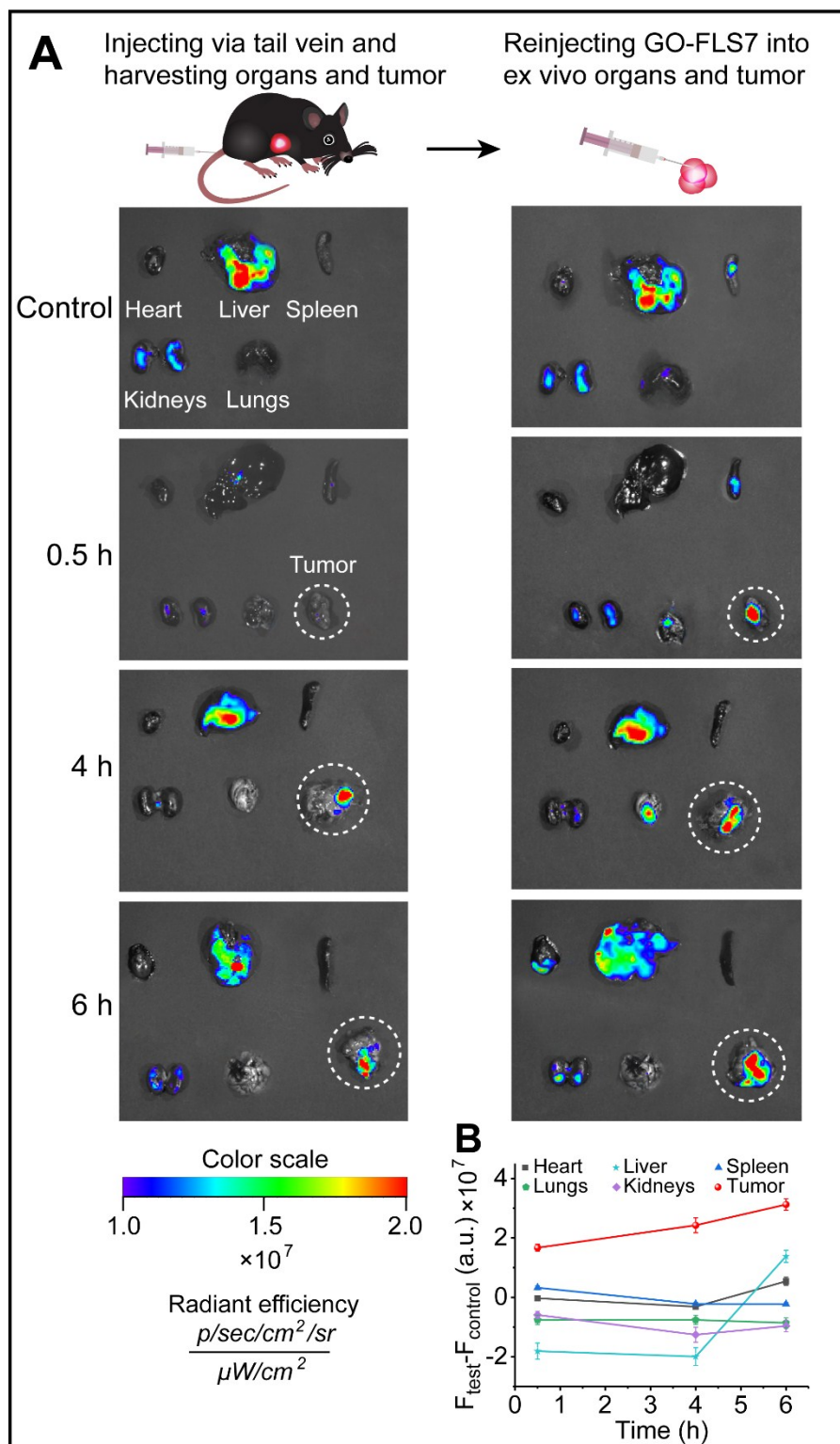


Figure S16. (A) Comparison of representative fluorescence images of ex vivo main organs (heart, liver, spleen, kidneys, and lungs) and tumor of tumor-bearing mice treated with GO-FLS7 complex at 0.5, 4, 6 h post-tail vein injection (left) and at 30 min post-reinjection of GO-FLS7 complex into ex

vivo organs and tumor (right). (B) Fluorescence intensity changes ($F_{\text{test}} - F_{\text{control}}$) of ex vivo organs and tumor at 30 min post-reinjection of GO-FLS7 complex (n = 3 samples). The results are presented as the mean \pm s.d.

References

1. Cho, J. H.; Kim, A. R.; Kim, S. H.; Lee, S. J.; Chung, H.; Yoon, M. Y., Development of a novel imaging agent using peptide-coated gold nanoparticles toward brain glioma stem cell marker CD133. *Acta Biomater.* **2017**, *47*, 182-192.
2. Wang, W.; Ma, Z.; Zhu, S.; Wan, H.; Yue, J.; Ma, H.; Ma, R.; Yang, Q.; Wang, Z.; Li, Q.; Qian, Y.; Yue, C.; Wang, Y.; Fan, L.; Zhong, Y.; Zhou, Y.; Gao, H.; Ruan, J.; Hu, Z.; Liang, Y.; Dai, H., Molecular Cancer Imaging in the Second Near-Infrared Window Using a Renal-Excreted NIR-II Fluorophore-Peptide Probe. *Adv. Mater.* **2018**, *30* (22), e1800106.
3. Shigdar, S.; Qiao, L.; Zhou, S.-F.; Xiang, D.; Wang, T.; Li, Y.; Lim, L. Y.; Kong, L.; Li, L.; Duan, W., RNA aptamers targeting cancer stem cell marker CD133. *Cancer Lett.* **2013**, *330* (1), 84-95.